Published in final edited form as:
Nat Ecol Evol. 2018 September ; 2(9): 1501–1506. doi:10.1038/s41559-018-0624-1.

The nature of aspidin and the evolutionary origin of bone

Joseph N. Keating[1,2], **Chloe L. Marquart**[1], **Federica Marone**[3], and **Philip C. J. Donoghue**[1]

[1]School of Earth Sciences, University of Bristol, Life Sciences Building, Tyndall Avenue, Bristol BS8 1TQ, UK [2]School of Earth and Environmental Sciences, University of Manchester, Michael Smith Building, Oxford Road, Manchester M13 9PT, UK [3]Swiss Light Source, Paul Scherrer Institut, CH-5232 Villigen, Switzerland

Abstract

Bone is the key innovation underpinning the evolution of the vertebrate skeleton, yet its origin is mired by debate over interpretation of the most primitive bone-like tissue, aspidin. This has variously been interpreted as cellular bone, acellular bone, dentine or as an intermediate of dentine and bone. The crux of the controversy is the nature of unmineralised spaces pervading the aspidin matrix, which have alternatively been interpreted as having housed cells, cell processes, or Sharpey's Fibres. Discriminating between these hypotheses has been hindered by the limits of traditional histological methods. Here we use Synchrotron X-ray Tomographic Microscopy (srXTM) to reveal the nature of aspidin. We show the spaces exhibit a linear morphology, incompatible with interpretations that they represent voids left by cells or cell processes. Instead, these spaces represent intrinsic collagen fibre bundles that form a scaffold, about which mineral was deposited. Aspidin is thus acellular dermal bone. We reject hypotheses that it is a type of dentine, cellular bone, or transitional tissue. Our study suggests the full repertoire of skeletal tissue types was established prior to the divergence of the earliest known skeletonising vertebrates, indicating that the corresponding cell types evolved rapidly following the divergence of cyclostomes and gnathostomes.

The origin of the vertebrate mineralised skeleton, and of its canonical suite of cell and tissue types, predates the radiation of crown gnathostomes. Fossil jawless vertebrates, assigned to the gnathostome stem, therefore provide a unique record of the evolutionary assembly of the vertebrate skeleton1. The Silurian-Devonian Heterostraci are of particular importance in this

Correspondence and requests for materials should be addressed to JNK and PCJD.

Author Contributions. J.N.K and P.C.J.D conceived the project. J.N.J and C.L.M processed the tomographic data. All authors contributed towards data collection, interpretation and writing the manuscript.

Competing interests. The authors declare no competing financial interests.

Additional information. Reprints and permissions information is available at www.nature.com/reprints. Publisher's note: Springer Nature remains neutral with regard to jurisdictional claims in published maps and institutional affiliations.

Data availability. The specimens on which this study was based are reposited at the Natural History Museum, London (NHMUK), Swedish Museum of Natural History (NRM-PAL) and the University of Bristol, School of Earth Sciences (BRSUG). The supporting tomographic datasets are available from the University of Bristol data repository (data.bris) at https://data.bris.ac.uk/data/dataset/1agbdxus79jan27rsyl580oxsp.

Europe PMC Funders Author Manuscripts

context, as they are considered among the most primitive skeletonising vertebrates (Fig. 1). Consequently, heterostracan skeletal biology is integral to elucidating the nature of the primitive vertebrate skeleton. Skeletal tissues of early vertebrates, including heterostracans, are preserved routinely in astonishing detail2, revealing cellular structure beyond the resolution of the most celebrated instances of exceptional preservation. Yet, in spite of this, the evolutionary significance of these ancient skeletons is obscured by controversy over the nature of the earliest bone-like tissue, aspidin. This controversy has, in turn, spilled into wider debate concerning the origin of the canonical repertoire of skeletal tissues. It has been argued that aspidin evidences an interval of plasticity between skeletal tissues, prior to the evolutionary differentiation of skeletal cell types3,4. In order to deduce the ancestral aspidin architecture, we studied taxa encompassing of the breadth of heterostracan diversity.

Hypotheses concerning the nature of aspidin hinge entirely upon interpretation of unmineralised spaces, which pervade the aspidin biomineral matrix (Fig. 2, 3). Correct interpretation of these structures requires characterisation of their 3-dimensional morphology and geometry within the aspidin matrix. Unfortunately, due to limitations inherent in 2-dimensional invasive histological methods, the spaces have been poorly characterised. For example, some researchers have distinguished coarse ‘spindle-shaped’ spaces from fine calibre ‘tubules’4–7, while others have made no distinction between spaces8–11. We used srXTM12–17, in addition to conventional invasive techniques, to characterise the histology of aspidin, as well as the 3-dimensional morphology and architecture of the spaces pervading through the tissue. These data permit direct histological comparison with the canonical skeletal tissues of living vertebrates, allowing us to test hypotheses concerning the identity of the aspidin spaces and, in turn, reveal the nature of this enigmatic tissue.

Results

The heterostracan cephalothoracic skeleton (Fig. 2a) is 4-layered (Fig. 2b, c), consisting of a superficial layer of dentine tubercles capped with enameloid, a compact reticular layer of canals (L1), a trabecular middle layer (L2) and a basal plywood-like layer of isopedin (L3), sometimes referred to as ‘lamellar aspidin’. It is important to note that the term ‘aspidin’ was initially conceived to describe only the middle layer of the heterostracan dermal skeleton10. However, its use has subsequently been expanded to describe seemingly acellular dermal skeletal tissues in galeaspids, thelodonts and anaspids, despite the fact that these tissues differ from aspidin *sensu stricto* both in terms of topology and histology8,11,18,19. We restrict the term aspidin to its original meaning, referring to the middle layer (L2) of the heterostracan cephalothoracic skeleton10. Aspidin developed around an extensive vascular network of anastomosing canals and/or interconnected polygonal cancellae (Fig. 2b, c). The cancellar trabecular walls are bipartite in construction (Fig. 3a, g, k), consisting of lamellar layers (next to the vascular lumina) and a homogenous biomineral core. The lamellar tissue developed centripetally, resulting in constriction of the vascular spaces11. The mineral matrix consists of elongate bundles (reflecting the fabric of the original collagen mesh) measuring 1-3μm in diameter, which form a circumferential interlaced fabric enveloping the vascular spaces (Figs. 3d, i, 4d).

Aspidin trabeculae are pervaded by unmineralised thread-like spaces, measuring approximately 2 – 5 μm in diameter and anywhere between 50 and >150 μm in length (Fig. 2d, 3a-k, 4a-c). These are preserved either as voids, or as diagenetic mineral infill. The spaces are linear; they do not bifurcate and show no ramifying processes (Fig. 4a). Within the trabecular walls, the spaces are oriented orthogonally to, and cross cut, the lamellar boundaries (Fig. 2d, 3, 4). Vertically, they are regularly spaced and are approximately parallel to each other. The spaces are more numerous and densely packed at the base of the vasculature, close to the boundary with the basal plywood layer (Fig. 2b). At intersections between trabecular walls, the linear spaces transect one another at 55-90°, forming an interwoven lattice (Figs. 2d, 3e, 4c-e). Similarly, in taxa with thick trabecular walls, such as *Tesseraspis*, the thread-like spaces pervading the homogenous core of the trabeculae are aligned parallel to the lamellar outer layers, transecting orthogonally aligned spaces (Fig. 4e).

Discussion

The aspidin spaces are incompatible with the interpretation that they represent cell spaces4,5,20–22 because they are strictly linear without ramifying processes, a key characteristic of osteocyte lacunae. They are not ‘spindle-shaped’ as has previously been suggested4,5,20,21, but instead comprise elongate threads with a consistent diameter over the course of their length. The perceived spindle-shape is an artefact of observing obliquely sectioned individual spaces, or else multiple overlapping spaces. They are also incompatible with osteocyte canuliculi, which are an order of magnitude smaller than the threads pervading the aspidin biomineral23. They are of comparable size to dentine tubules, yet dentine is topologically incompatible with aspidin. The former is primarily a superficial dermal skeletal tissue, although it is occasionally deployed as a secondary mineralization tissue5, while the latter makes up the primary tissue of the middle layer of the heterostracan skeleton. Morphological comparison between ‘true’ dentinal tubules, found in the tubercles decorating the surface of heterostracan dermal armour, and the aspidin spaces shows they differ markedly.

Of the competing interpretations of the aspidin spaces, only collagen is morphologically compatible. These spaces are far too coarse to have housed individual fibres, yet they are of comparable size to collagen fibre bundles in mineralised tissues of living vertebrates24. Two types of fibre bundle are found in the dermal skeleton, termed extrinsic (i.e. Sharpey’s Fibres) and intrinsic. Extrinsic fibre bundles function as attachment structures anchoring the dermal skeleton to the periosteum25. As such, they tend to be concentrated at the margins of mineralised elements and rarely penetrate deeper into the skeleton. Indeed, extrinsic fibre bundles are associated with the basal plywood layer of the heterostracan dermal skeleton and are typically coarser, longer and less densely packed than aspidin fibre bundle spaces (Fig. 2b). Intrinsic collagen fibres, on the other hand, are ubiquitous throughout dermal bone. In teleost acellular bone, intrinsic collagen fibres form bundles cross-cutting the contiguous lamellae of the mineralised matrix, in much the same manner as the aspidin spaces. These are unmineralised in life, and so form voids in the mineral matrix post-mortem26. The aspidin spaces are organised radially about cancellae and orthogonal to the circumferential mineralised collagen bundles (Fig 2d, 4a-c), or else tangled at the boundaries between

cancellae. They do not extend through the basal layer or superficial layer and, thus, could not have been used as attachment fibres to anchor the skeleton within the dermis. However, their organisation is entirely compatible with intrinsic collagen. Cells migrating through a collagen mesh have been shown to organise fibres in two axes parallel and orthogonal to their migrating trajectory27,28. Tensile forces induced by migrating fibroblasts organise collagen into ‘straps’ parallel to the course of cell migration27. However, due to the nonlinear properties of collagen meshes, fibres are reorganised perpendicular to the migration direction in a process known as orthogonal amplification of mesh distortion28. Thus, aspidin structure suggests that, prior to mineralisation, the collagen mesh is reorganised via cell migration, resulting in a circumferential fabric of straps parallel to the fibroblast migration, as well as an orthogonal fabric of straps propagated by mesh distortion. The orthogonal straps together form an intrinsic scaffold of unmineralised collagen, about which mineralisation of the mesh occurs.

Identification of aspidin spaces as voids housing unmineralised collagen permits reconsideration of aspidin homology and its significance in understanding the origin and early evolution of the vertebrate mineralised skeleton. Hypotheses that aspidin represents a type of dentine8 or intermediate between dentine and bone6 are based entirely upon interpretation of the aspidin spaces as canuliculi, comparable to dentine tubules, which we have falsified. Rather, the histology of aspidin is entirely compatible with bone. Specifically, aspidin is topologically compatible with trabecular bone, i.e. diploë comprising the intermediate layer of the dermatocranium of crown gnathostomes. Contra 4,5,20–22, we show that aspidin is acellular, in the sense that it contains no cell lacunae. There has been much debate over the primacy of cellular vs. acellular bone, largely stemming from the fact that both bone types appear simultaneously in the fossil record3. However, ancestral state reconstruction allows us to resolve this controversy, revealing acellularity as the plesiomorphic condition, with cellular bone evolving from an acellular bone independently on at least two occasions: in the lineage leading to osteostracans and jawed vertebrates, and within pteraspidomorphs29 (Figure 1).

Identification of aspidin as acellular bone eliminates the last piece of evidence that early vertebrates exhibit a high degree of skeletal plasticity prior to differentiation of the canonical suite of skeletal tissues. Instead, our results, together with previous research2,7–11,30, suggest that acellular bone, dentine and enameloid were already established prior to the divergence of the known skeletonising vertebrate clades. These tissue types appear simultaneously in the fossil record, and in topological co-ordination, without any precursor. One possible explanation for this punctuated appearance is that it records the evolutionary innovation of biomineralisation. It has been suggested that many of the key genes responsible for synthesis of collagenous tissues emerged through duplication associated with whole genome duplication (WGD) events early in vertebrate evolution, and redundant copies were subsequently co-opted for biomineralisation31,32. The origin of biomineralisation has also been linked to the evolution of secretory calcium-binding phophoprotein (SCPP) genes via tandem duplication following WGD. Unfortunately the relative and absolute timing of early vertebrate WGD is poorly understood. Conventionally, two rounds of WGD are inferred to have occurred, either prior to33, or either side of34, the divergence of cyclostomes and gnathostomes. More recent analysis of the lamprey germline genome casts

doubt on these scenarios, preferring instead a single WGD proceeded by a series of large segmental duplications35,36. Additional insight from hagfish and elasmobranch genomes will help resolve the tempo of vertebrae genomic evolution and provide a test for hypotheses concerning the punctuated appearance of mineralised tissues in the fossil record.

The nature of aspidin has proved elusive since it was first described over 80 years ago. We show that the unmineralised aspidin spaces, which have provoked such controversy, are best interpreted as a scaffold of collagen fibre bundles, about which mineral was deposited. These spaces are aligned orthogonal to a radial fabric of mineralised fibre bundles, which circumscribe the polygonal cancellae. The organisation of these fabrics is consistent with orthogonal amplification of mesh distortion via osteoblasts migration. These data identify aspidin as acellular dermal bone. Hypotheses that it comprises a cellular type of bone, a type of dentine, or an intermediate tissue grade are rejected. Our study suggests that the full repertoire of skeletal cell and tissue types was already established in the earliest known skeletonising vertebrates (Figure 1); a consequence of expansion of neural crest cell fates following the divergence of cyclostomes and gnathostomes37.

Methods

The material of this study originates from a number of geological localities. *Lepidaspis serrata* and *Pteraspis* sp. material is from the Drake Bay Formation of Prince of Wales Island in the Canadian Arctic Archipelago and is stored at the Naturhistoriska Riksmuseet, Stockholm (NRM). The *Tesseraspis tesselata*, *Phialaspis symondsi*, *Corvaspis kingi* and *Anglaspis macculloughi* material is from a small stream section at Earnstrey Hall Farm, Shropshire, UK and is stored at the Natural History Museum, London (NHM). *Loricopteraspis dairydinglensis* is from a stream section in nearby Dairy Dingle and is also stored at the NHM and at the University of Bristol. *Rhinopteraspis crouchi* material is from Cradley, Herefordshire and is stored at the NHM. The *Poraspis* sp. material comes from Jagilnytsia Stara, Podolia, Ukraine, and is stored at the NHM. The *Psammosteus megalopteryx* specimen was received from the collection of the late Beverly Halstead and is of unknown provenance. It has been accessioned at the NHM.

Scanning Electron Microscopy

Specimens were embedded using Struers EpoFix® resin and left to cure for at least 24 h. Sections were cut using a Buehler IsoMet® low speed saw. Cut surfaces were impregnated using Buehler EPO THIN® resin. Small specimens were then mounted in 25 mm diameter aluminium rings using Buehler EpoFix®. All specimens were ground manually using P800 to P4000 grit paper. Buehler IsoCut Fluid was used for lubrication during grinding. Large sections were polished manually using Buehler MetaDi® 3 and 1 μm Diamond Paste. Following 24h curing, specimens were ground manually using P1200 to P4000 grit paper. Specimens mounted in aluminium rings were polished using a Buehler Ecomet® 250 Grinder–Polisher using Buehler MetaDi® 3 and 1μm suspensions. Selected polished sections were etched using 5% orthophosphoric acid (H_3PO_4) for between 1 -2 minutes. Polished specimens were carbon coated using the Emitech K450 carbon coater. Images were

taken using a Hitachi S-3500N SEM. SEM analysis was conducted at the University of Bristol School of Earth Science's Electron Microbeam Facility.

Light Microscopy

LM thin sections were examined using a Leica M205C microscope with a 2X Plan Apochromat lens and imaged with a Leica DFC425C digital camera. Sections were analysed using both Bright-Field and Nomarski Differential Interference Contrast (DIC) microscopy.

Synchrotron Radiation X-Ray Tomographic Microscopy

SrXTM experiments were conducted at the X04SA-MS and X02DA-TOMCAT beamlines of the Swiss Light Source, Paul-Scherrer Institut, Villigen, Switzerland. Measurements were taken using 10x and 20x objective lenses, 13-25 keV, and 180–2500 ms exposure times. For each dataset, 1501 equiangular projections were acquired over 180 degrees. These were postprocessed and rearranged into flat- and dark-field-corrected sinograms. Reconstruction was performed on a Linux PC cluster using a highly optimised routine based on the Fourier transform method and a regridding procedure, resulting in volumetric data with voxel dimensions of 0.65 μm (10x objective) and 0.325 μm (20x objective). The data were analysed in Aviso 8.0. Tomographic sections were produced using the orthoslice module. Virtual thin sections were produced using the volume rendering module.. The data were cropped producing thin sections 10–100 slices thick. Aspidin vasculature and spaces were modelled using the virtual segmentation module.

Supplementary Material

Refer to Web version on PubMed Central for supplementary material.

Acknowledgments

We thank John Cunningham (University of Bristol), Martin Rucklin (Naturalis, Leiden) and Carlos Martinez-Perez (University of Valencia) for beamline assistance and Stuart Kearns (University of Bristol) for his assistance at the Bristol Earth Sciences Microprobe Facility. We thank Georgy Koentges (University of Warwick) and Ivan Sansom (University of Birmingham) for discussion. JNK was funded by a NERC Studentship. PCJD is funded by NERC (NE/P013678/1; NE/N002067/1; NE/G016623/1) and BBSRC (BB/N000919/1). CLM completed this work in partial fulfilment of the MSc Palaeobiology at the University of Bristol.

References

1. Donoghue PCJ, Keating JN. Early vertebrate evolution. Palaeontology. 2014; 57:879–893.
2. Donoghue PCJ, Sansom IJ. Origin and early evolution of vertebrate skeletonization. Microscopy Research and Technique. 2002; 59:352–372. DOI: 10.1002/jemt.10217 [PubMed: 12430166]
3. Smith MM, Hall BK. Development and evolutionary origins of vertebrate skeletogenic and odontogenic tissues. Biological Reviews. 1990; 65:277–373. [PubMed: 2205303]
4. Halstead LB. Calcified tissues in the earliest vertebrates. Calcified Tissue International. 1969; 3:107–124.
5. Halstead Tarlo LB. Psammosteiformes (Agnatha) - A review with descriptions of new material from the Lower Devonian of Poland. I - General part. Palaeontologia Polonica. 1964; 13:1–135.
6. Halstead LB. The heterostracan fishes. Biological Reviews. 1973; 48:279–332.
7. Ørvig T. Histologic studies of ostracoderms, placoderms and fossil elasmobranchs. 6. Hard tissues of Ordovician vertebrates. Zoologica Scripta. 1989; 18:427–446.

8. Denison RH. Ordovician vertebrates from Western United States. Fieldiana Geology. 1967; 16:131–192.
9. Bystrow AP. The microstructure of skeleton elements in some vertebrates from lower Devonian deposits of the USSR. Acta Zoologica. 1959; 40:59–83.
10. Gross W. Die fische des mittleren Old Red Südlivlands. Geologische und Palaeontologische Abhandlungen. 1930; 18:123–156.
11. Gross W. Histologische studien am aussenskelett fossiler agnathen und Fische. Palaeontographica Abteilung A. 1935; 83:1–60.
12. Donoghue PCJ, et al. Synchrotron X-ray tomographic microscopy of fossil embryos. Nature. 2006; 442:680–683. [PubMed: 16900198]
13. Tafforeau P, et al. Applications of X-ray synchrotron microtomography for non-destructive 3D studies of paleontological specimens. Applied Physics a-Materials Science & Processing. 2006; 83:195–202.
14. Rucklin M, et al. Development of teeth and jaws in the earliest jawed vertebrates. Nature. 2012; 491:748–753. [PubMed: 23075852]
15. Sanchez S, Ahlberg PE, Trinajstic KM, Mirone A, Tafforeau P. Three-dimensional synchrotron virtual paleohistology: a new insight into the world of fossil bone microstructures. Microscopy and Microanalysis. 2012; 18:1095–1105. [PubMed: 23026256]
16. Qu Q, Blom H, Sanchez S, Ahlberg P. Three-dimensional virtual histology of silurian osteostracan scales revealed by synchrotron radiation microtomography. Journal of morphology. 2015; 276:873–888. [PubMed: 25809461]
17. Keating JN, Donoghue PCJ. Histology and affinity of anaspids, and the early evolution of the vertebrate dermal skeleton. Proceedings of the Royal Society of London B: Biological Sciences. 2016; 283doi: 10.1098/rspb.2015.2917
18. Märss T. A new Late Silurian or early Devonian thelodont from the Boothia Peninsula, Arctic Canada. Palaeontology. 1999; 42:1079–1099.
19. Zhu M, Janvier P. The histological structure of the endoskeleton in galeaspids (Galeaspida, Vertebrata). Journal of Vertebrate Paleontology. 1998; 18:650–654.
20. Rohon JV. Die obersilurischen fische von Oesel. Mem Acad Sci St Petersbourg; 1893.
21. Halstead Tarlo LB. Aspidin: the precursor of bone. Nature. 1963; 199:46–48. [PubMed: 14047939]
22. Novitskaya LI. Psammosteids (Agnatha, Psammosteidae) of the Devonian of the USSR. Obruchev D, Mark-Kurik E, editorsGeological Institute of the Estonian Academy of Sciences; 1966. 257–282.
23. You LD, Weinbaum S, Cowin SC, Schaffler MB. Ultrastructure of the osteocyte process and its pericellular matrix. The Anatomical Record Part A: Discoveries in Molecular, Cellular, and Evolutionary Biology. 2004; 278:505–513.
24. Höhling H, Kreilos R, Neubauer G, Boyde A. Electron microscopy and electron microscopical measurements of collagen mineralization in hard tissues. Zeitschrift für Zellforschung und Mikroskopische Anatomie. 1971; 122:36–52. [PubMed: 5122599]
25. Aaron JE. Periosteal Sharpey's fibers: a novel bone matrix regulatory system. Frontiers in endocrinology. 2012; 3:1–10. [PubMed: 22649402]
26. Moss ML. The biology of acellular teleost fish bone. Annals of the New York Academy of Sciences. 1963; 109:337–350. [PubMed: 13936210]
27. Petroll WM, Cavanagh HD, Jester JV. Dynamic three-dimensional visualization of collagen matrix remodeling and cytoskeletal organization in living corneal fibroblasts. Scanning. 2004; 26:1–10. [PubMed: 15000286]
28. Sawhney RK, Howard J. Slow local movements of collagen fibers by fibroblasts drive the rapid global self-organization of collagen gels. The Journal of cell biology. 2002; 157:1083–1092. [PubMed: 12058022]
29. Sansom IJ, Haines PW, Andreev P, Nicoll RS. A new pteraspidomorph from the Nibil Formation (Katian, Late Ordovician) of the Canning Basin, Western Australia. Journal of Vertebrate Paleontology. 2013; 33:764–769.

30. Keating JN, Marquart CL, Donoghue PCJ. Histology of the heterostracan dermal skeleton: Insight into the origin of the vertebrate mineralised skeleton. Journal of morphology. 2015; 276:657–680. [PubMed: 25829358]

31. Kawasaki K, Buchanan AV, Weiss KM. Biomineralization in humans: making the hard choices in life. Annual review of genetics. 2009; 43:119–142.

32. Huxley-Jones J, Robertson DL, Boot-Handford RP. On the origins of the extracellular matrix in vertebrates. Matrix Biology. 2007; 26:2–11. [PubMed: 17055232]

33. Kuraku S, Meyer A, Kuratani S. Timing of genome duplications relative to the origin of the vertebrates: did cyclostomes diverge before or after? Molecular biology and evolution. 2009; 26:47–59. [PubMed: 18842688]

34. Holland PW, Garcia-Fernàndez J, Williams NA, Sidow A. Gene duplications and the origins of vertebrate development. Development. 1994; 1994:125–133.

35. Smith JJ, Keinath MC. The sea lamprey meiotic map improves resolution of ancient vertebrate genome duplications. Genome research. 2015; 25:1081–1090. [PubMed: 26048246]

36. Smith JJ, et al. The sea lamprey germline genome provides insights into programmed genome rearrangement and vertebrate evolution. Nat Genet. 2018; 50:270–277. DOI: 10.1038/s41588-017-0036-1 [PubMed: 29358652]

37. Donoghue PCJ, Graham A, Kelsh RN. The origin and evolution of the neural crest. BioEssays. 2008; 30:530–541. [PubMed: 18478530]

Europe PMC Funders Author Manuscripts

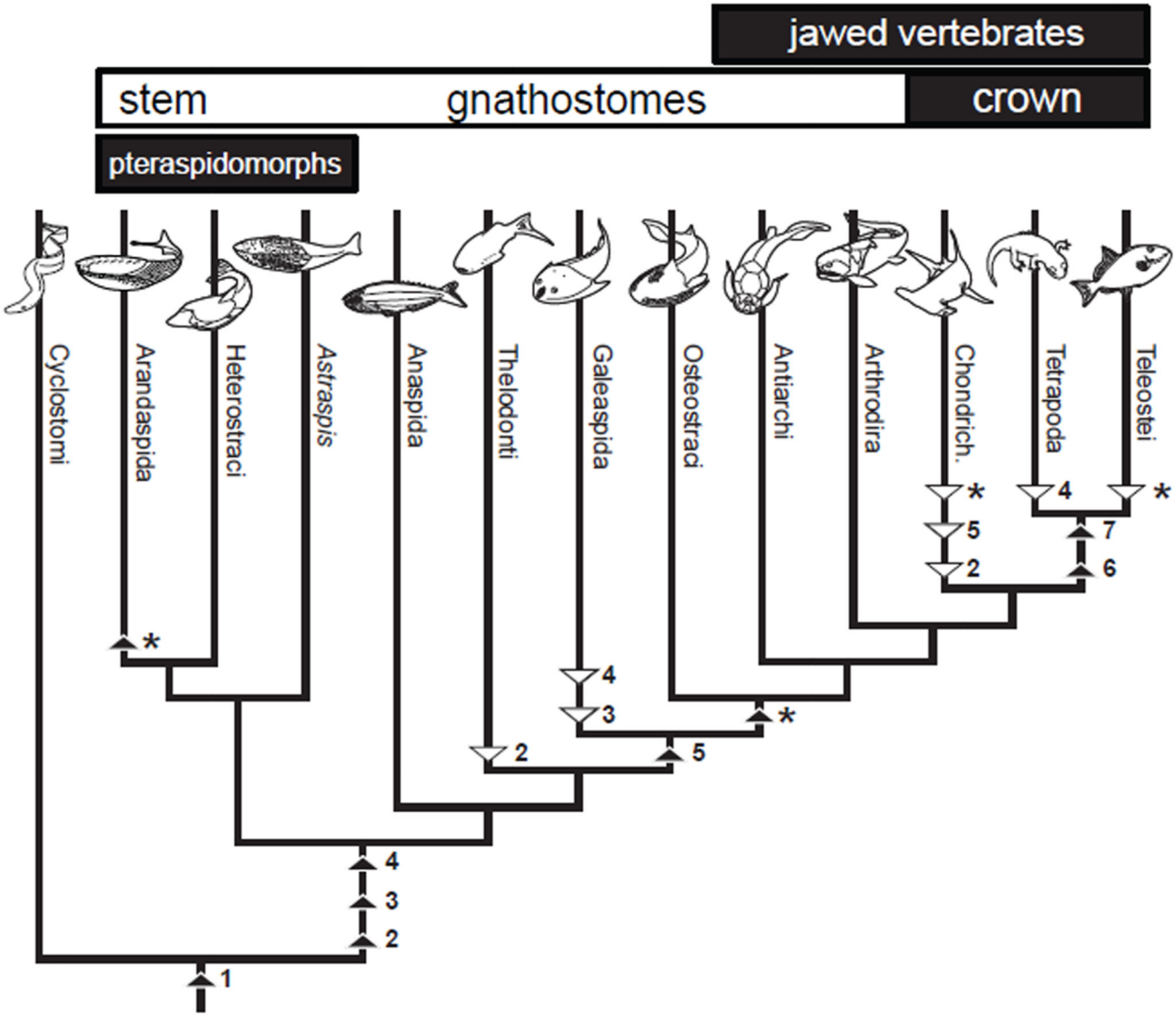

Figure 1. Hypothesis of vertebrate relations based on Keating & Donoghue17.

Heterostracans, together with the Ordovician aged Arandaspids and Astraspis comprise the clade Pteraspidomorpha, interpreted as the sister group to all other ostracoderms + crown gnathostomes (i.e. all other skeletonising vertebrates). Based on our histological analyses we inferred character evolution using parsimony. Black triangles represent character gain and white triangles represent character loss. Cartilage (1), dermal bone (2), dentine (3), enameloid (4), perichondral bone (5), endochondral bone (6), enamel (7), cell spaces in dermal bone (*).

Europe PMC Funders Author Manuscripts

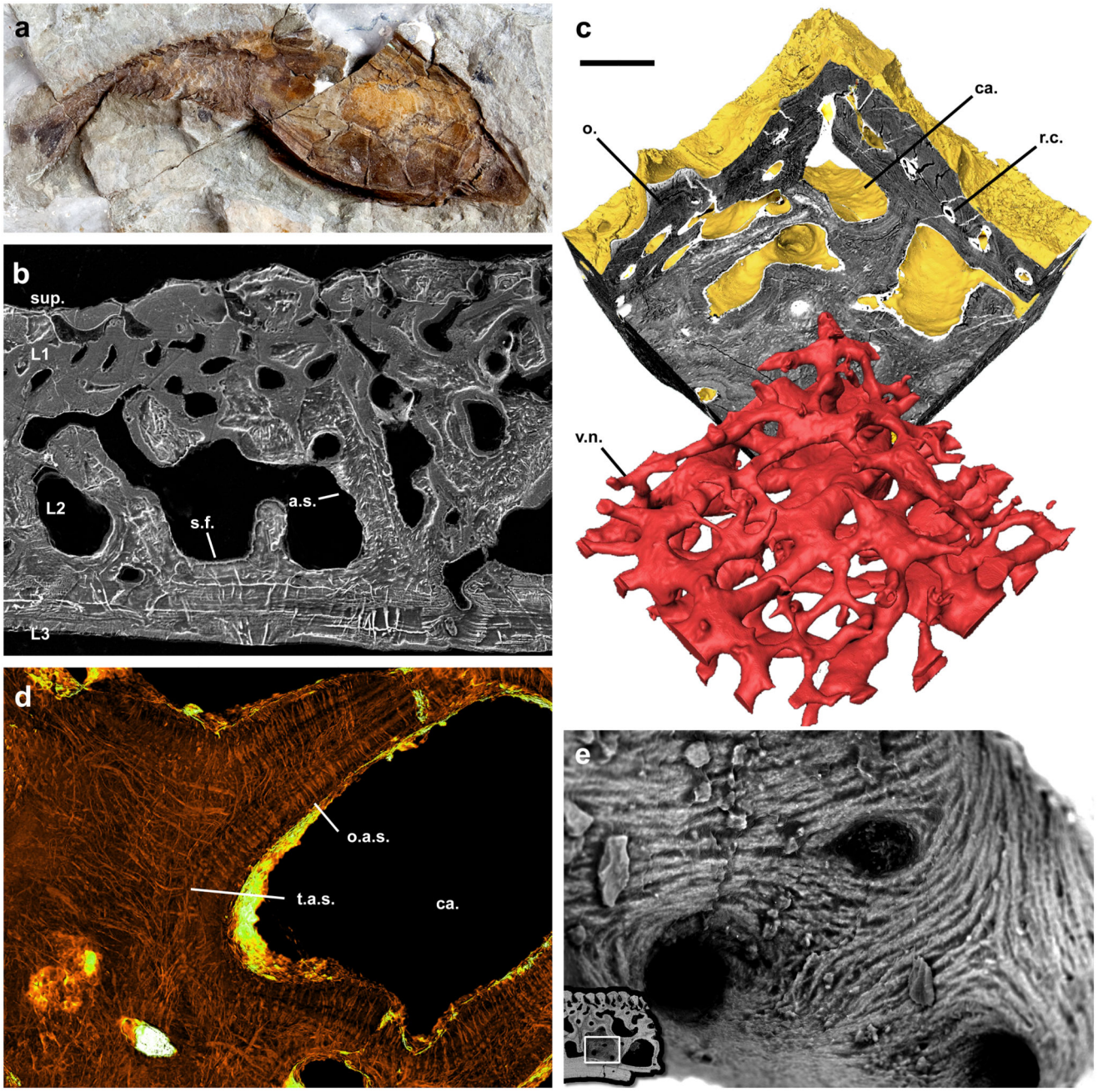

Figure 2. Morphology and histology of the heterostracan dermal skeleton.

Gross external morphology of the dermal skeleton of *Errivaspis waynensis* (NHMUK P19789) from the Lochkovian of Herefordshire, UK (a); etched SEM section of *Loricopteraspis dairydinglensis* (NHMUK P75400) showing the 4-layered construction of the dermal skeleton. Aspidin spaces and Sharpey's Fibre spaces are preserved as high relief pyrite diagenetic infill. Sharpey's Fibre spaces pervading L3 can be distinguished from aspidin spaces in L2 by both their size and configuration (b); sectioned srXTM virtual model of the dermal skeleton of *Tesseraspis tesselata* (NHMUK P73617). The vasculature network

is shown to comprise a series cancellae interlinked by reticular canals (c); SrXTM horizontal virtual thin section through aspidin trabeculae of *Tesseraspis tesselata* (NHMUK P73618). Aspidin spaces are preserved as diagenetic pyrite infill with high X-ray attenuation. Spaces are organised orthogonal to the trabecular lamellae, or else tangled at trabecular intersections (d); SEM detail of a cancellar chamber of *Loricopteraspis dairydinglensis* (NHMUK P73622), showing a centripetal fabric of coarse spicules, interpreted as mineralised (crystal) fibre bundles (e); SrXTM horizontal virtual thin section through aspidin trabeculae of *Tesseraspis tesselata* (NHMUK P73618). Aspidin spaces are preserved as diagenetic pyrite infill with high X-ray attenuation. Spaces are organised orthogonal to the trabecular lamellae, or else tangled at trabecular intersections (e). r.c., reticular canal; o., odontode; v.n., vascular network; ca, cancellae; a.s., aspidin space; o.a.s., orthogonal aspidin space; t.a.s., tangled aspidin space; s.f., Sharpey's Fibre space; sup, superficial layer; L1, layer 1; L2, layer 2; L3, layer 3. Relative scale bar equals 21mm in (a), 183 μm in (b), 165 μm in (c), 83 μm in (d). and 49 μm in (e).

Europe PMC Funders Author Manuscripts

Europe PMC Funders Author Manuscripts

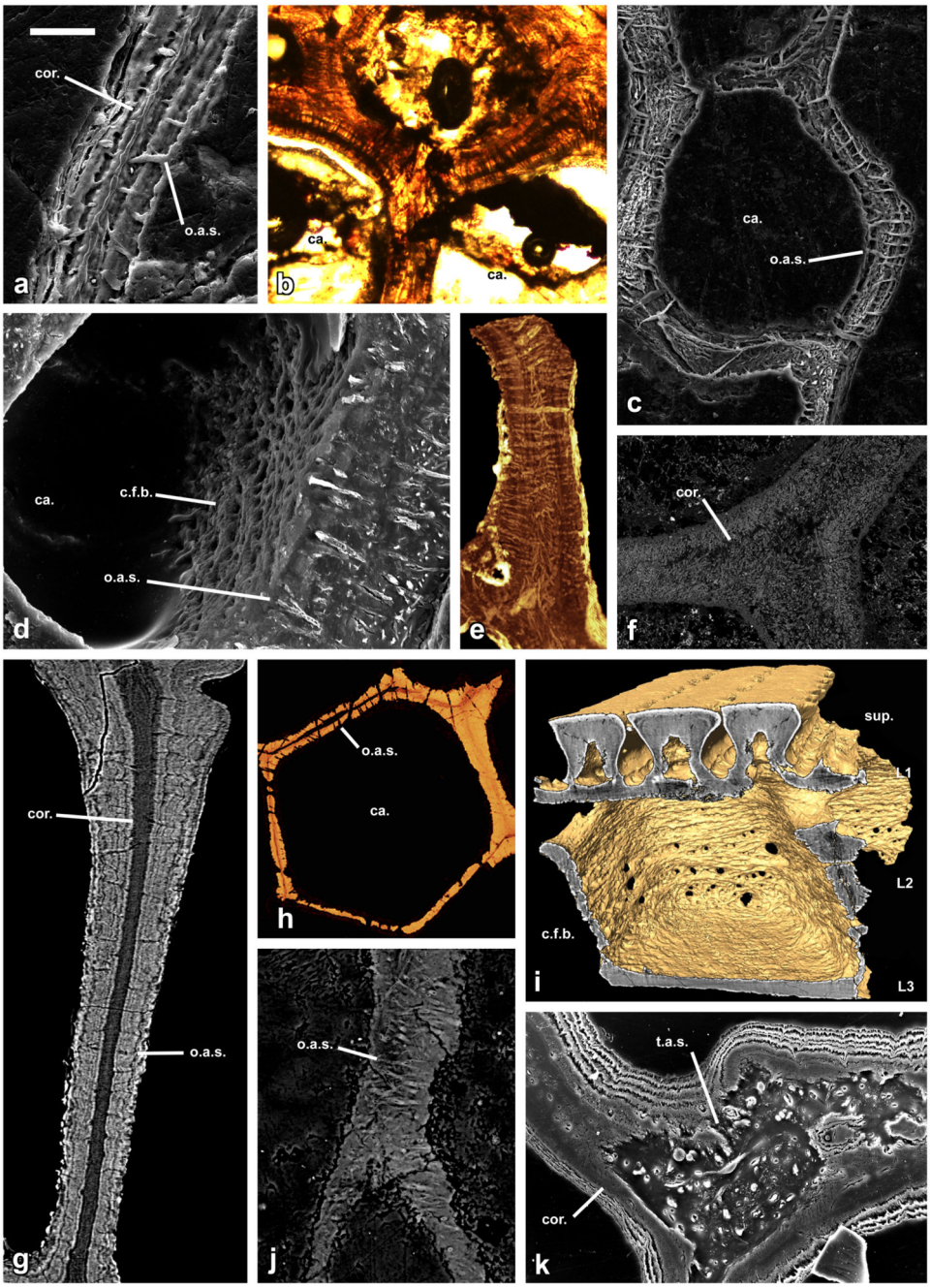

Figure 3. Histology of aspidin in phylogenetically disparate heterostracan taxa.

SEM etched section of a trabecular wall of *Lepidaspis serrata* NRM-PAL C.5940 showing bipartite construction (a); LM thin section of a junction of trabecular walls of *Phialaspis symondsi* NHMUK P73619 (b); etched SEM section through a polygonal cancellar chamber of *Corvaspis kingi* NHMUK P73616 (c); BSE SEM vertical section through a polygonal cancellar chamber of *Corvaspis kingi* NHMUK P73613 showing both the aspidin spaces and rystal fibre bundles (d); horizontal SrXTM virtual thin section through trabecular walls of *Tesseraspis tesselata* NHMUK P73617 (e); SEM BSE section of a trabecular junction of

Amphiaspis sp. GIT 313-32 (f); SrXTM tomographic slice through a vertical trabecular of *Anglaspis macculloughi* NHMUK P73620 (g); SrXTM horizontal virtual thin section through a polygonal cancellar chamber of *Pteraspis* sp. NRM-PAL C.5945 (h); isosurface model of the same specimen showing the circular fabric of fibres enveloping the cancellae (i); vertical trabecular wall of *Poraspis* sp. NHMUK P17957 (j); junction of trabecular walls of *Loricopteraspis dairydinglensis* NHMUK P73623 (k). sup, superficial layer; L1, layer 1; L2, layer 2; L3, layer 3; ca, cancellae; o.a.s., orthogonal aspidin space; t.a.s., tangled aspidin space; c.f.b., crystal fibre bundles; cor., homogenous core of bipartite aspidin trabeculae. Relative scale bar equals 30 μm in (a), 48 μm in (b), 79 μm in (c), 30 μm in (d), 88 μm in (e), 180 μm in (f), 41 μm in (g), 100 μm in (h), 91 μm in (i), 40 μm in (j) and 52 μm in (k).

Europe PMC Funders Author Manuscripts

Europe PMC Funders Author Manuscripts

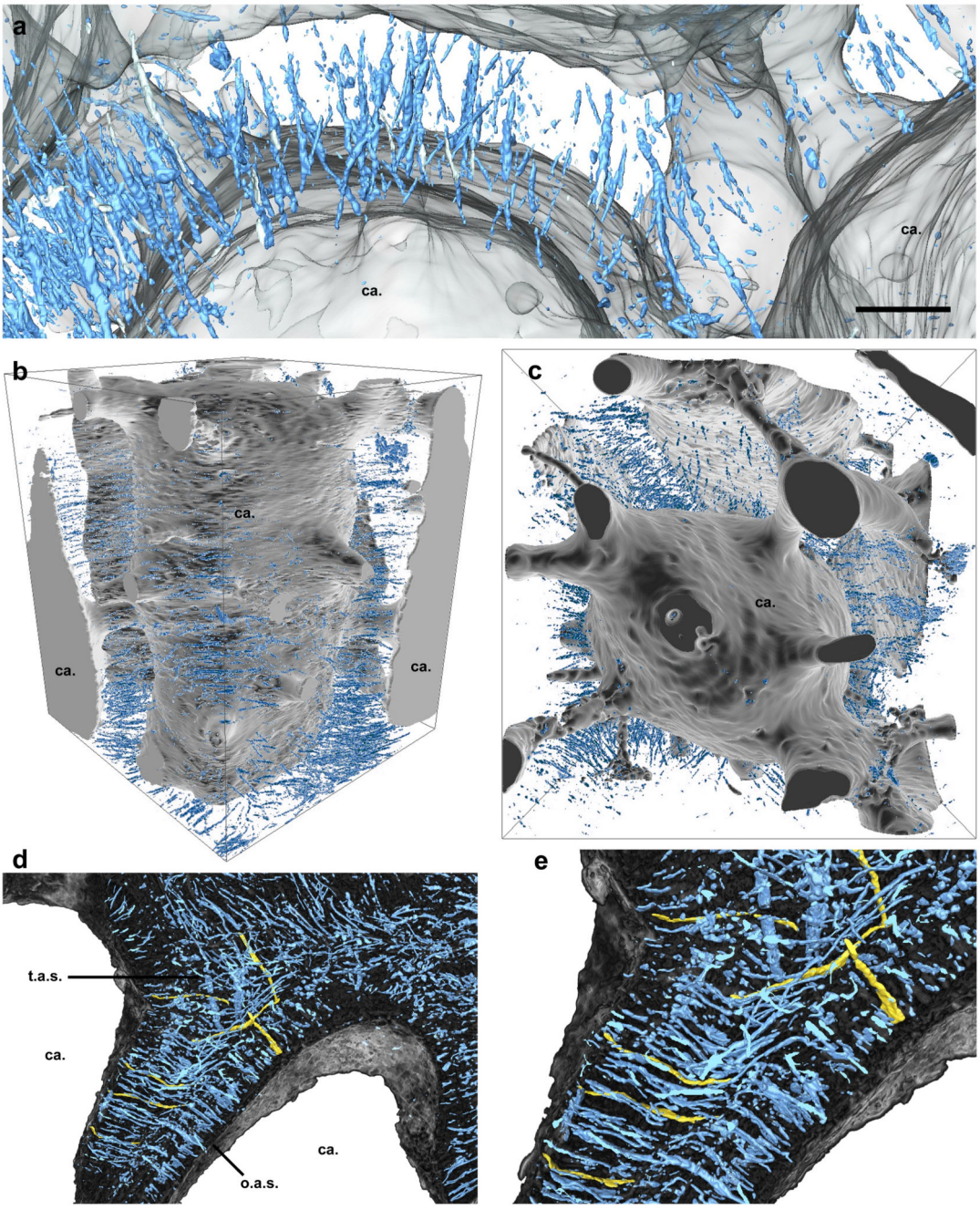

Figure 4. SrXTM virtual segmentation of aspidin spaces in *Loricopteraspis dairydinglensis* (NHMUK P75401) (a-c) and *Tesseraspis tesselata* (NHMUK P73617) (d, e).

Detail of orthogonal aspidin spaces pervading the trabecular walls dividing polygonal cancellae. These spaces exhibit linear morphology without ramifications, precluding interpretation that these are cell or cell process spaces (a); lateral (b), and transverse (c) views of the organisation of aspidin spaces radiating about a polygonal cancellar vacuity; Horizontal section of the middle layer of *Tesseraspis tesselata* showing orthogonal aspidin spaces within the trabeculae and tangled aspidin spaces at the intersection between trabeculae. Several orthogonal and tangled spaces have been segmented individually

(highlighted in gold) to illustrate their linear, non-branching morphology (d), Detail of previous panel (e). Relative scale bar equals 55 μm in (a), 189 μm in (b) 160 μm in (c), 92 μm in (d) and 50 μm in (e).

Europe PMC Funders Author Manuscripts